Supporting information for Journal of Materials Chemistry C

Circularly polarized light emission from chiral nematic phenylterthiophene dimer exhibiting ambipolar carrier transport

Taichi Hamamoto and Masahiro Funahashi*

Department of Advanced Materials Science, Faculty of Engineering, Kagawa University

Hole transport of chiral phenylquaterhiophene dimer

Figure S1 exhibits the molecular structure of phenylquaterthiophene derivative **1** bearing a binaphthyl group. Compound **1** was synthesized according to the literature.[1)] Compound **1** exhibits a chiral nematic phase below 155 ºC and a glass transition is observed at 52 ºC.

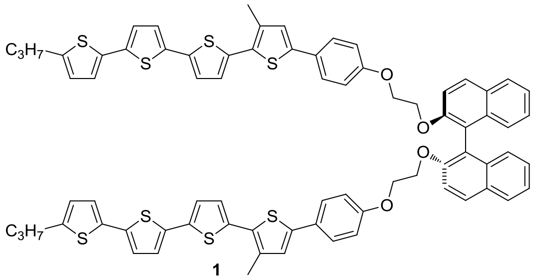

Fig. S1 Molecular structure of phenylquaterthiophene derivative **1** bearing a binaphthyl group.

The carrier mobility in the chiral nematic phase was measured by a time-of-flight method. Figure S2 displays transient photocurrent curves for positive charge carriers in the chiral nematic phase at 70 ºC. For negative charges, photocurrent was so weak that their mobility could not be determined. For positive charges, photocurrent signals influenced by space charges were obtained and the hole mobility was determined. The hole mobility was strongly dependent on the electric field and the temperature. At 70 ºC, the hole mobility was 7×10^{-6} $cm^2V^{-1}s^{-1}$ at the electric field of 1.1×10^5 Vcm^{-1} and 4×10^{-6} $cm^2V^{-1}s^{-1}$ at 7.8×10^4 Vcm^{-1}. Above 80 ºC, stable and strong photocurrent response was not obtained because of the increase in the dark current, and the hole mobility could not be determined.

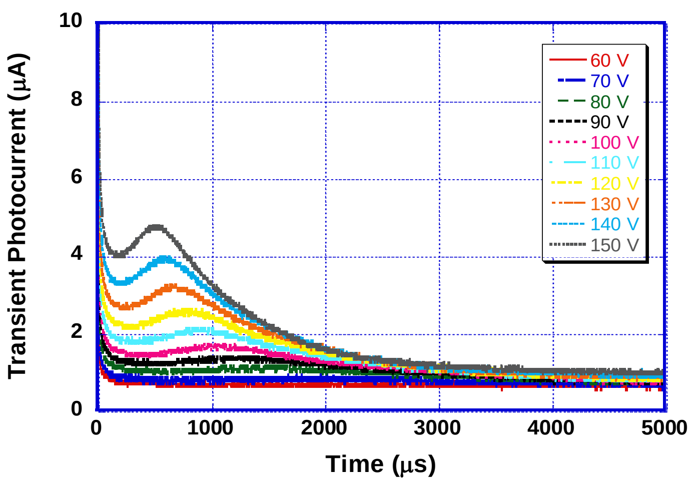

Figure S2 Transient photocurrent curves for holes in the chiral nematic phase of compound **1** at 70 ºC. The sample thickness is 9 μm.

1) M. Funahashi, N. Tamaoki, *Mol. Cryst. Liq. Cryst.*, 2007, **475**, 123-135.

^{1}H NMR spectra of (S)-PD and (R)-PD

^{1}H NMR spectra were measured in $CDCl_3$ solution using a Varian UNITY INOVA 400NB spectrometer. These spectra were completely identical.

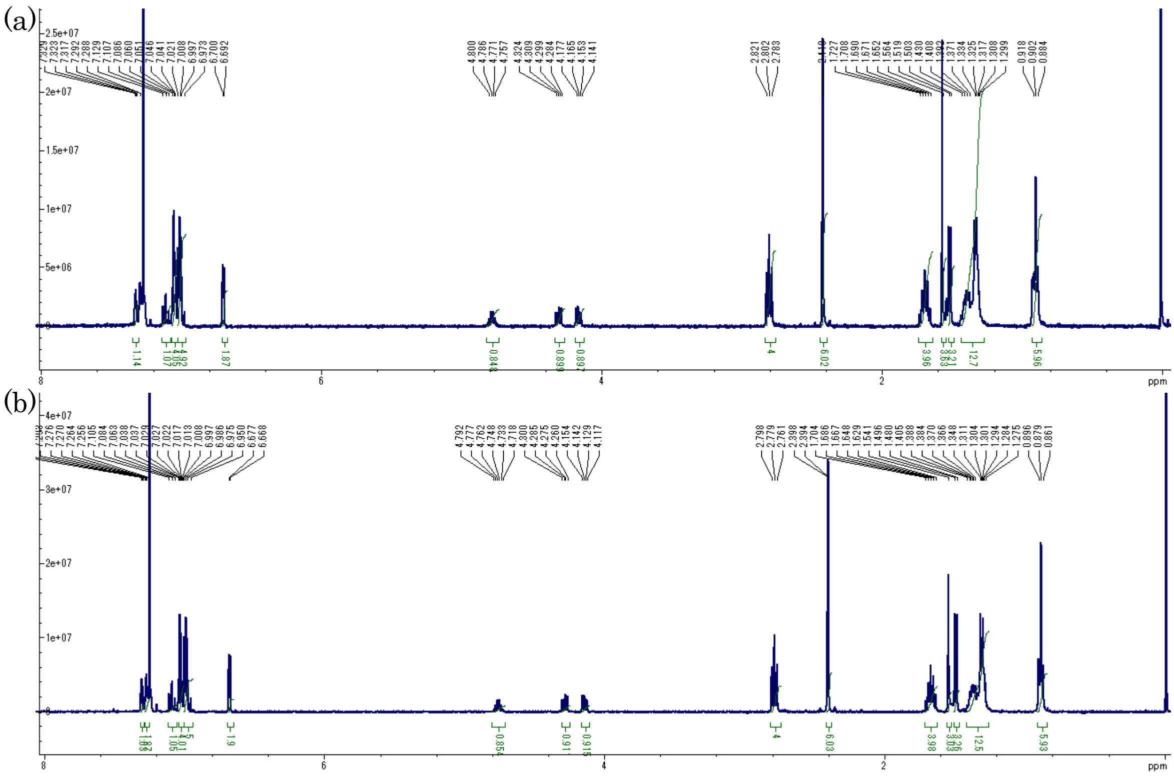

Figure S3 ^{1}H NMR spectra of (a) (S)-**PD** and (b) (R)-**PD**

Mesomorphic property of (R)-PD and a mixture of (S)- and (R)-PD

Figures S4 exhibit DSC thermograms of pure (R)-PD and a 1:2 mixture of (S)- and (R)-PD. The phase transition temperatures and transition enthalpies of (S)-PD, (R)-PD, and the mixture are basically identical.

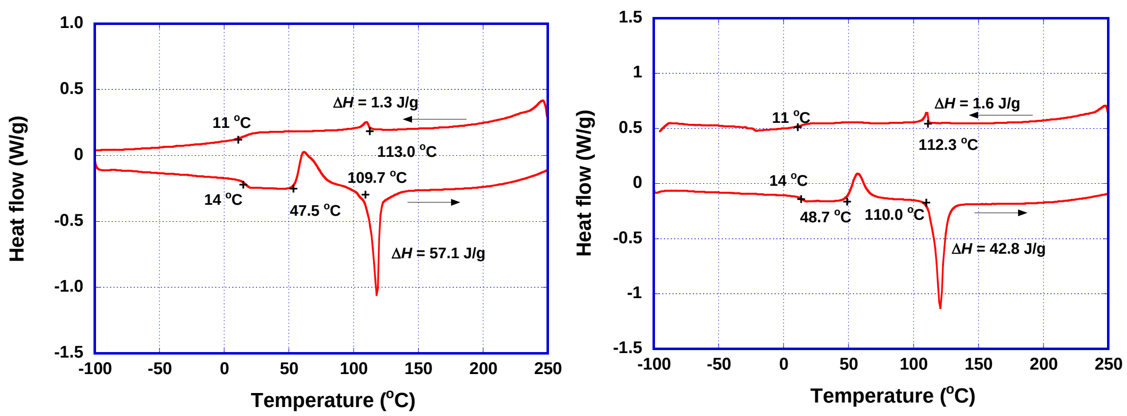

Figure S4 DSC thermograms of (a) (R)-**PD** and a 1:2 mixture of (S)- and (R)-**PD**

Figure S5 exhibits polarizing optical micrographic textures of (R)-**PD** and a 1:2 mixture of (S)- and (R)-**PD**. The optical texture is identical with that of (S)-**PD**. When the sample was cooled from the isotropic to the chiral nematic phase, focal conic texture was obtained. Shearing the sample in the chiral nematic phase, the helical axes oriented parallel to the substrate. In the 1:2 mixture of (S)- and (R)-**PD**, the optical texture after the application of the shearing stress was colored green because of the selective reflection of the chiral nematic phase.

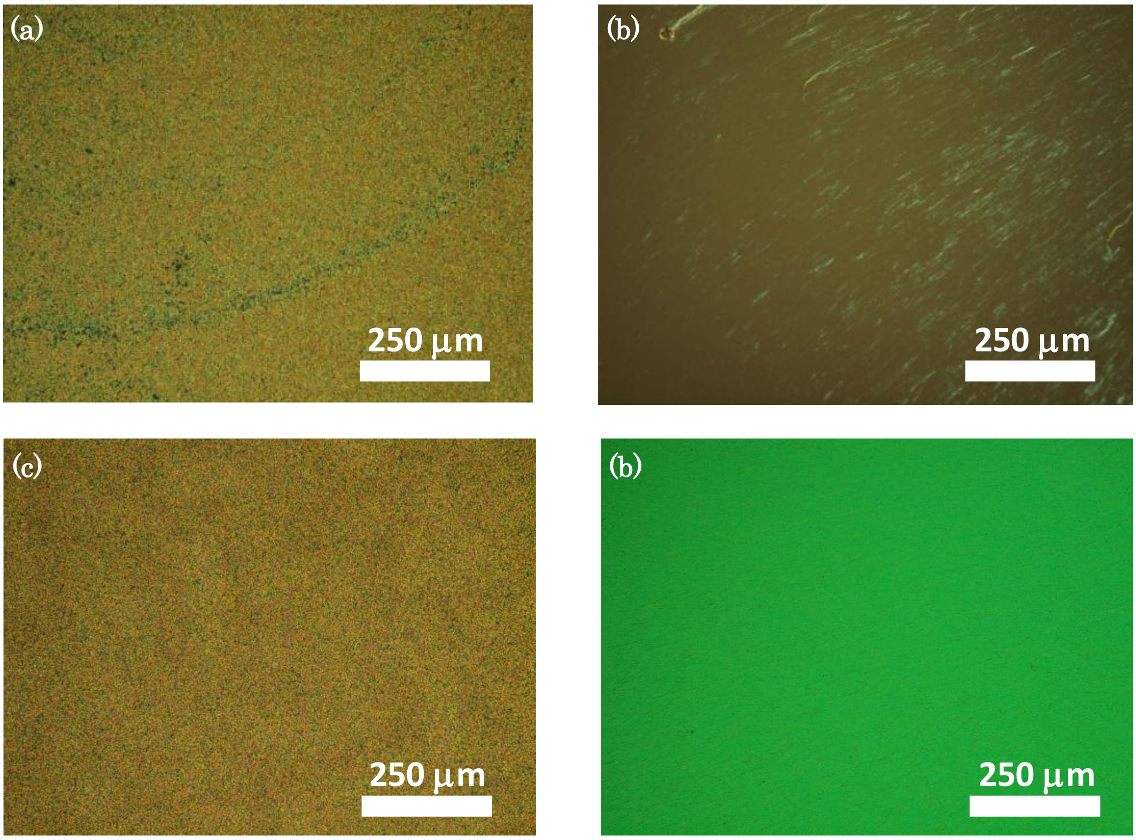

Figure S5 Optical micrographic textures of a sample of (a) (R)-**PD** during cooling process at 100 ºC, (b) after sharing stress at 100 ºC, (c) 1:2 mixture of (S)- and (R)-**PD** at 100 ºC, and (d) after sharing stress at 100 ºC.

Carrier transport characteristics of (R)-PD and a 1:2 mixture of (S)- and (R)-PD

Carrier mobilities in the chiral nematic phases of compound (R)-**PD** and a 1:2 mixture of (S)- and (R)-**PD** were determined by a time-of-flight (TOF) method. Figure S6 exhibits transient photocurrent curves for holes and electrons in the chiral nematic phase of (R)-**PD**. The hole and electro mobilities were identical with those in the chiral nematic phase of (S)-**PD**. The temperature- and field-dependences were also same as those of (S)-**PD**.

Figure S7 exhibits transient photocurrent curves for holes and electrons in the chiral nematic phase of a 1:2 mixture of (S)- and (R)-**PD**. The hole and electron mobilities were identical with those in the chiral nematic phase of pure (S)- and (R)-**PD**. The temperature- and field-dependences were also same as those of pure (S)- and (R)-**PD**.

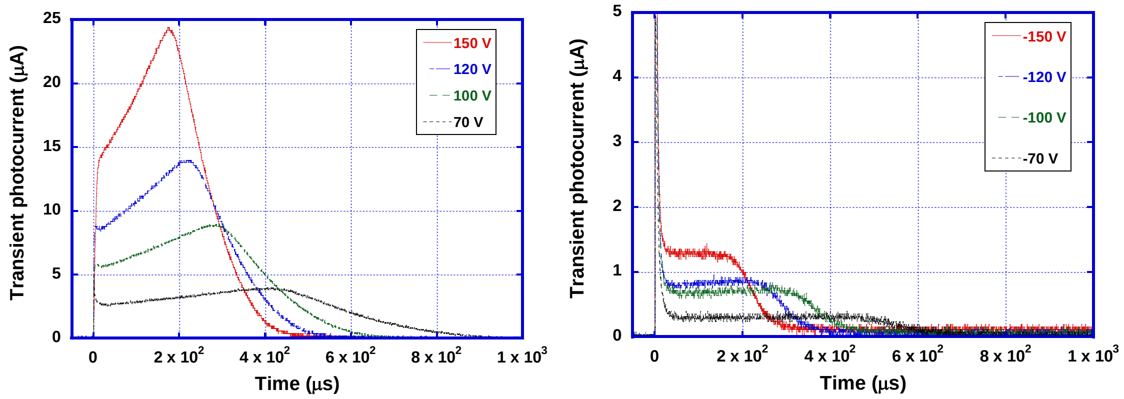

Figure S6 Transient photocurrent curves in the chiral nematic phase of (R)-**PD** at 100 ºC for (a) holes and (b) electrons. The sample thickness was 9 μm and the wavelength of the excitation light was 356 nm.

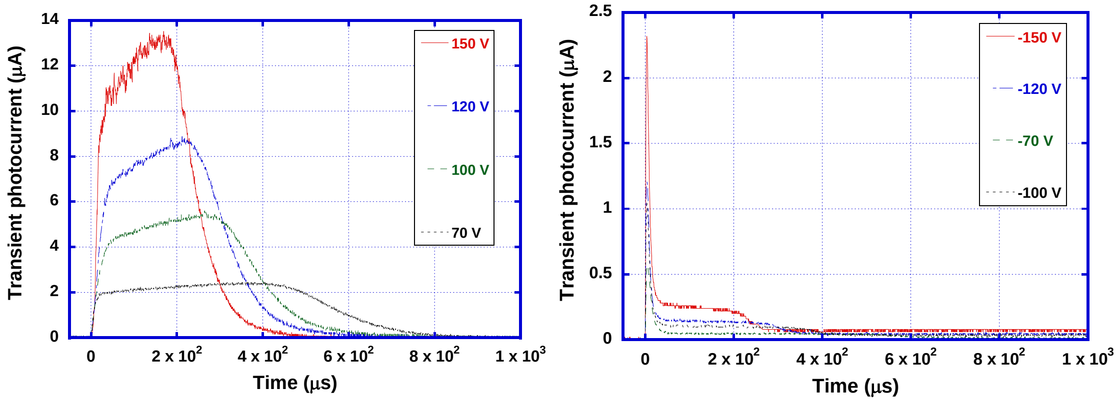

Figure S7 Transient photocurrent curves in the chiral nematic phase of a 1:2 mixture of (R)- and (S)-**PD** at 100 ºC for (a) holes and (b) electrons. The sample thickness was 9 μm and the wavelength of the excitation light was 356 nm.